



HAL
open science

Analysis of thigh muscle stiffness from childhood to adulthood using magnetic resonance elastography (MRE) technique

Laëtitia Debernard, Ludovic Robert, Fabrice Charleux, Sabine F Bensamoun

► To cite this version:

Laëtitia Debernard, Ludovic Robert, Fabrice Charleux, Sabine F Bensamoun. Analysis of thigh muscle stiffness from childhood to adulthood using magnetic resonance elastography (MRE) technique. *Clinical Biomechanics*, 2011, 26 (8), pp.836-840. 10.1016/j.clinbiomech.2011.04.004 . hal-03811589

HAL Id: hal-03811589

<https://utc.hal.science/hal-03811589v1>

Submitted on 12 Oct 2022

HAL is a multi-disciplinary open access archive for the deposit and dissemination of scientific research documents, whether they are published or not. The documents may come from teaching and research institutions in France or abroad, or from public or private research centers.

L'archive ouverte pluridisciplinaire **HAL**, est destinée au dépôt et à la diffusion de documents scientifiques de niveau recherche, publiés ou non, émanant des établissements d'enseignement et de recherche français ou étrangers, des laboratoires publics ou privés.

1 **Analysis of thigh muscle stiffness from childhood to adulthood using**
2 **Magnetic Resonance Elastography (MRE) technique**

3
4 Laëtitia Debernard, PhD¹
5 Ludovic Robert, Mr²
6 Fabrice Charleux, MD²
7 Sabine F. Bensamoun, PhD¹
8

9 ¹Biomechanics and Bioengineering Laboratory, UMR CNRS 6600, Université de
10 Technologie de Compiègne, Compiègne, France

11 ²ACRIM-Polyclinique Saint Côme, Compiègne, France
12

13
14 *Paper*

15
16 *Word count: 2913*

17
18 *6 figures*

19
20 *21 references*
21
22
23
24
25
26

27 **Corresponding Author:**

28 Sabine Bensamoun, Ph.D.

29 Université de Technologie de Compiègne (UTC)
30 Centre de Recherches de Royallieu
31 Laboratoire de Biomécanique et Bioingénierie, UMR CNRS 6600
32 BP 20529
33 Rue Personne de Roberval
34 60205 Compiègne cedex
35 France
36 Tel: 33 3 44 23 43 90
37 Email: sabine.bensamoun@utc.fr
38

39

40 **ABSTRACT**

41 *Background:* Magnetic resonance elastography (MRE) was performed in healthy and
42 pathological muscles in order to provide quantitative muscle stiffness data to clinicians.
43 Moreover, due to the lack of data on muscle children, the present work studies age-
44 related changes of the mechanical properties from childhood to adulthood.

45 *Methods:* 26 healthy subjects composed of 7 children (8-12 years), 9 young adults (24-29
46 years) and 10 middle-aged adults (53-58 years) underwent a MRE test. Shear modulus
47 (μ) and its spatial distribution, as well as the attenuation coefficient (α) were measured on
48 the vastus medialis muscle at rest and at contracted conditions (10% and 20% of the
49 maximum voluntary contraction) for each group.

50 *Findings:* The shear modulus linearly increases with the degree of contraction for young
51 adults while it is maximum at 10 % of the maximum voluntary contraction (MVC) for
52 children ($\mu_{\text{children}_{10\%}} = 14.9$ kPa (SD 2.18)) and middle-aged adults ($\mu_{\text{middle-aged}_{10\%}} =$
53 10.42 kPa (SD 1.38)). Mapping of shear modulus revealed a diffuse distribution of colors
54 reflecting differences in muscle contractile properties as a function of age. Moreover, the
55 attenuation coefficient showed a similar behavior for all groups, i.e. a decrease from the
56 relaxed state to 10 % MVC followed by a plateau at 20% MVC.

57 *Interpretation:* This study demonstrates that the MRE technique is sensitive enough to
58 detect changes in mechanical properties from childhood to adulthood and has the
59 potential to determine muscle mechanical properties for patients suffering from
60 neuromuscular disorders, particularly during therapeutic trials.

61
62 Key words: shear modulus map, age, muscle growth, magnetic resonance elastography

INTRODUCTION63
64
65

Muscle tissue is strongly utilized throughout life during daily activity, exercise or physical work inducing different muscle efforts. Muscles pathologies such as myopathy detected in childhood, fibromyalgia present in adult muscles or muscle weakness exhibited by older individuals can also alter the muscle stiffness and its morphological properties. Thus, a complete understanding of the morphological and mechanical properties of muscle will allow for the development of muscle prevention.

71
72
73
74
75
76
77
78
79
80
81
82
83
84
85

As a consequence of the morphological changes, the mechanical properties of muscle are also affected. Most of the studies (e.g. Akima et al., 2001; Lynch et al., 1999) used an isokinetic dynamometer to measure peak torque during knee extension and flexion, or concentric and eccentric elbow movements. All of these analyses showed a gradually decrease of the mechanical parameters, from 20 to 85 years of age for men and for women. Since 2001, magnetic resonance elastography (MRE) technique has also been used to characterize *in vivo* mechanical properties of healthy and diseased muscle (Dresner et al., 2001; Basford et al., 2002; Bensamoun et al., 2006, 2007; Brauck et al., 2007). This technique analyzed the propagation of shear waves inside the muscle allowing for the measurement of shear modulus which is related to the muscle function. Indeed, MRE was performed on patients with lower-extremity neuromuscular dysfunction (Basford et al., 2002), hyperthyroidy (Bensamoun et al., 2007) and fibromyalgia (Chen et al., 2007, 2008) in order to establish a muscle stiffness data base for the follow up of patient and the effect of treatment. Furthermore, Domire et al. (2009a) have analyzed the standard deviation of the shear modulus to investigate the muscle

86 tissue homogeneity and a relationship was found between the age (from 50 to 70 years of
87 age) and the tissue homogeneity for the tibialis anterior muscle.

88 In addition to the shear modulus, MRE technique provides a wave attenuation
89 coefficient as a measure of muscle quality (Domire et al., 2009b). Most of muscle MRE
90 studies were performed on adult's muscles, from 20 to 80 years of age, but there is a lack
91 of data characterizing the mechanical properties of muscle for children. This study is the
92 first to show the capability of the MRE technique to measure children muscle stiffness.
93 Morphological properties were widely quantified by ultrasound studies on healthy
94 children in order to be compared with children affected by neuromuscular disorders
95 (Kamala et al., 1985; Heckmatt et al., 1988; Lamminen et al., 1988; Schedel et al., 1992;
96 Schmidt et al., 1993; Zuberi et al., 1999; Pillen et al., 2007).

97 The purpose of this study is to characterize the vastus medialis mechanical
98 properties at different muscle conditions for children, young adults and middle-aged
99 adults. Moreover, the originality of this present work is to introduce for the first time the
100 evolution of the shear modulus map related to the level of contraction.

101 MATERIALS AND METHODS

102 Participants

103 Seven prepubescent children (6 males and 1 female, mean age = 10.9 yrs (SD
104 0.6), range = 8-12, mean Body Mass Index: BMI = 17.3 (SD 0.9)), nine young adults (5
105 males and 4 females, mean age = 26.4 yrs (SD 1.7), range = 24-29, mean BMI = 23.69
106 (SD 3.34)) and ten middle-aged adults (3 males and 7 females, mean age = 55.2 yrs (SD
107 2.39), range = 52-58, mean BMI = 26.39 (SD 4.72)) without muscle abnormality and no
108 history of muscle disease underwent a MRE test. These three age points have been
109 chosen to represent different muscle states corresponding to the muscle growing phase
110 (children), a mature muscle (young adult) and the first beginning of aging muscle
111 (middle-aged adults). This study has been approved by the institutional review board and
112 informed consents were obtained from adult participants and from the parents for minor
113 volunteers.

114

115 Experimental setup for magnetic resonance elastography (MRE) technique

116

117 The subject lays supine on an adult leg press (Bensamoun et al., 2006) which was
118 adapted for children's size. The knee was flexed to 30° with the right foot placed on a
119 footplate, in which a load cell (SCAIME, Annemasse, France) was fixed to record the
120 developed force and a visual feedback (LABVIEW program) of the applied load is given
121 to the volunteers inside the MR room. Then, a pneumatic driver consisting of a remote
122 pressure driver connected to a long hose was wrapped and clamped around the subject's

123 thigh and a custom-made Helmholtz surface coil was placed around the thigh. Shear
124 waves were induced through the thigh muscles at 90Hz (*f*).

125 MRE experiments were performed for each subject on the VM muscle, in the
126 relaxed and contracted (10% and 20% of the maximum voluntary contraction: MVC)
127 states reflecting the muscular activity of the quadriceps muscle. A delay (few minutes)
128 between individual experiments was given to the volunteers in order to avoid fatigability
129 effects. This procedure was repeated in the same condition, at different times, on few
130 subjects for the different age groups.

131

132 **Magnetic resonance elastography (MRE) tests**

133 Axial image of the thigh muscle was acquired with a gradient echo sequence (1.5T
134 General Electric HDxt MRI) in order to place an oblique scan plane on the medial side of
135 the thigh to visualize the vastus medialis muscle. Then, MRE images were collected with
136 a 256 x 64 acquisition matrix (interpolated to 256 x 256), a flip angle of 45°, a 24 cm
137 field of view and a slice thickness of 5 mm. Four offsets were recorded with the vastus
138 medialis (VM) muscle in relaxed and contracted (10%, 20% MVC) states during a scan
139 time of 52 seconds using a TR/TE of 100 ms/23 ms.

140

141 **Image processing and data analysis**

142 MRE technique provides anatomical image of the VM muscle (Fig. 1a) as well as
143 phase image (Fig. 1b) showing the shear wave displacement within the muscle. A white
144 profile was manually placed in the direction of the wave propagation that follows the

145 orientation of the fascicle paths as previously demonstrated (Debernard et al., 2011). The
146 quantification of the wavelength (λ) along this profile leads to the measurement of the
147 local shear modulus ($\mu_{\text{local}} = \rho\lambda^2f^2$, with $\rho = 1000 \text{ kg/m}^3$ for the muscle density)
148 assuming that the muscle is linearly elastic, locally homogeneous, isotropic and
149 incompressible.

150 Attenuation coefficient (α) of the shear wave displacement was measured along
151 the prescribed white profile. This parameter is obtained from a Fourier Transform of the
152 distance covered by each pixel during the four offsets (Domire et al., 2009b). The
153 amplitude value of the first temporal harmonic of each pixel was extracted at the driven
154 frequency 90Hz providing the amplitude displacement image (Fig. 1c). Then, a curve
155 representing the shear wave displacement amplitude according to the distance (sampling
156 step corresponding to the pixel size: 0.9mm) was obtained and fitted with an exponential
157 function $Ae^{-(\alpha d)}$, with the parameters “A” and “d” representing the displacement
158 amplitude value and the distance along the profile, respectively (Fig. 2).

159 A map of the shear modulus was generated from the wave displacement image
160 using the local frequency estimate (LFE) algorithm (Manduca et al., 2001) providing a
161 spatial distribution of the muscle shear modulus. Assuming that muscle tissue is locally
162 homogeneous, an ellipsoid region of interest (ROI) was placed around the prescribed
163 profile in order to quantify a more important muscle stiffness area reflected by a global
164 shear modulus (μ_{ROI}) compared to the local one (μ_{local}) measured along the profile.

165

166

167

168 Statistical analysis

169 The statistical analysis was performed with the software Statgraphics 5.0 (Sigma Plus,
170 Maryland, USA) using a two-factor ANOVA (age, muscle state) and when P values were
171 significant post hoc t -test (Student-Newman-Keuls) were done. The effects of age and
172 muscle state were determined on shear modulus and attenuation coefficient. The
173 significance was fixed to $P < 0.05$.

174

175 RESULTS

176 Effects of muscle condition (relaxed or contracted) on shear modulus and attenuation 177 coefficient for children, young adults and middle-aged adults.

178 Young adults showed a significant ($P<0.01$) linear increase of the shear modulus from
179 the relaxed ($\mu_{\text{young}} = 3.83$ kPa (SD 0.24)) to 20% MVC ($\mu_{\text{young}} = 12.97$ kPa (SD 0.87)),
180 whereas the children and older individuals showed only a significant ($P<0.01$) increase
181 between the relaxed ($\mu_{\text{children}} = 2.99$ kPa (SD 0.19), $\mu_{\text{middle-aged}} = 3.84$ kPa (SD 0.42)) and
182 10% MVC ($\mu_{\text{children}} = 14.90$ kPa (SD 2.18), $\mu_{\text{middle-aged}} = 10.42$ kPa (SD 1.38)) (Fig. 3a, 3b).
183 We note that children revealed the highest increase of shear modulus (5 fold) from the relaxed
184 to the contracted (10% MVC) state (Fig. 4a), whereas the young and middle-aged adults
185 showed a lower increase of muscle shear modulus (about 2 fold) (Fig. 4b, Fig. 4c). Between
186 10% and 20% MVC, individuals in their fifties revealed a slightly decrease ($\mu_{\text{middle-aged}_{10\%}}$
187 MVC = 10.42 kPa (SD 1.38), $\mu_{\text{middle-aged}_{20\%}}$ MVC = 9.13 kPa (SD 1.19)) (Fig. 4c), compared to
188 the young adults which continue to increase their shear modulus with the same ratio (2 fold)
189 (Fig. 4b).

190 The reproducibility of the shear modulus was measured as the standard deviation (SD)
191 from the repeated MRE tests. The SD measurements were ± 0.32 kPa and 0.45 kPa in relaxed
192 and contracted conditions for all groups, respectively.

193 The effect of the muscle condition (relaxed or contracted) on the shear wave
194 attenuation was the same for the three age groups. Thus, children, young and middle-aged
195 adults showed a significant ($P<0.05$) decrease of 34.72 m⁻¹ (SD 3.13), 18.75 m⁻¹ (SD 0.93)
196 and 12.00 m⁻¹ (SD 1.64) between the relaxed state and 10% of MVC, respectively (Fig. 5a-
197 5b). In agreement with the shear modulus results, children showed the most important

198 attenuation from the relaxed to contracted (10% MVC) condition. Then, the attenuation
199 coefficient is consistently maintained from 10% to 20% of MVC for all the groups.

200 **Effect of age on the muscle shear modulus and attenuation coefficient for the relaxed** 201 **and contracted positions**

202 In a relaxed state, the children had a slightly ($P<0.01$) lower shear modulus ($\mu_{\text{children}} =$
203 2.99 kPa (SD 0.19)) compared to adult's groups which have similar shear modulus ($\mu_{\text{young}} =$
204 3.83 kPa (SD 0.24), $\mu_{\text{middle-aged}} = 3.84$ kPa (SD 0.42)) (Fig. 3b).

205 At 10% of MVC, the highest significant difference ($P<0.05$) of shear modulus was
206 found between the children and young adults (about 7.6 kPa) while a smaller difference ($P<$
207 0.01) was found between the adult's groups (about 3 kPa). However, no difference was found
208 between children and middle-aged adults, probably due to the large range of shear modulus
209 measured for children. At 20% of MVC, only a significant ($P<0.01$) difference of shear
210 modulus was found between adult's groups.

211 The only effect of age on the shear wave attenuation was found when the muscle was
212 relaxed (Fig. 5a). Indeed, children revealed a significant ($P<0.05$) difference with young
213 adults (about 13 m^{-1}) (Fig. 5a). The results demonstrate any effect of age on the shear wave
214 attenuation when the muscle was contracted.

215 **Cartography of stiffness**

216 Figure 6 illustrates the shear modulus map and the corresponding anatomical image
217 obtained for the children, young and middle-aged subjects when the VM muscle was at rest
218 and at contracted positions (10% and 20% of MVC). At rest, the shear modulus map for the
219 three groups showed a homogeneous purple color in the region of interest (ROI) (Fig. 6a, Fig.
220 6d, Fig. 6g) placed around the red profile where the shear modulus was locally quantified.

221 The comparison of the shear modulus measured inside the ROI ($\mu_{\text{children}} = 3.61$ kPa (SD
222 0.27), $\mu_{\text{young}} = 4.14$ kPa (SD 0.26), $\mu_{\text{middle-aged}} = 3.2$ kPa (SD 0.48)) and along the red profile
223 ($\mu_{\text{children}} = 2.99$ kPa (SD 0.19), $\mu_{\text{young}} = 3.83$ kPa (SD 0.24), $\mu_{\text{middle-aged}} = 3.84$ kPa (SD
224 0.42)) was in the same range.

225 When the VM muscle was contracted, the shear modulus map exhibited a diffuse
226 distribution of colors, around the region of interest (Fig. 6b-6c, Fig. 6e-6f, Fig. 6h-6i),
227 demonstrating that the shear waves were sensitive to the muscle media and more specifically
228 to the contraction of the muscle fibers. At 10% MVC, children showed the highest shear
229 modulus value locally measured along the profile and is well represented on the shear
230 modulus map ($\mu_{\text{local}} = 14.9$ (SD 2.02) vs $\mu_{\text{ROI}} = 12.4$ (SD 1.36)) with a distribution of stiffer
231 tissues inside the ROI (Fig. 6b) in response to the muscle contraction. For the same level of
232 contraction (10% MVC) stiffer muscle tissue showed up inside the ROI for children (Fig 6b)
233 ($\mu_{\text{ROI}} = 12.4$ (SD 1.36)) compared to adult groups ($\mu_{\text{ROI}} = 9.08$ (SD 2.29)) (Fig. 6e-6h).
234 Moreover, this result is in agreement with the highest shear modulus measured locally along
235 the white profile for children ($\mu_{\text{local}} = 14.9$ kPa (SD 2.02)) compared to adult groups (μ_{local}
236 $= 8.88$ kPa (SD 2.18)). At 20% MVC, young adults (Fig.6f) exhibited stiffer muscle tissue
237 around the region of interest ($\mu_{\text{ROI}} = 11.9$ kPa (SD 1.38)) compared to the mapping obtained
238 at 10% MVC ($\mu_{\text{ROI}} = 7.46$ kPa (SD 0.85)) (Fig. 6e). This result is in agreement with the
239 linear increase of shear modulus previously found between 10% ($\mu_{\text{local}} = 7.33$ kPa (SD 1.23))
240 and 20% MVC ($\mu_{\text{local}} = 12.97$ kPa (SD 0.87)). At the opposite, middle-aged participants
241 showed a mapping with less stiff tissue around the ROI at 20% MVC ($\mu_{\text{ROI}} = 8.53$ kPa (SD
242 2.01)) (Fig. 6i) than 10% MVC ($\mu_{\text{ROI}} = 10.7$ kPa (SD 2.06)) (Fig 6h), confirming the slight
243 decrease of the shear modulus locally measured at 10% MVC ($\mu_{\text{local}} = 10.42$ kPa (SD 1.38))
244 and at 20% MVC ($\mu_{\text{local}} = 9.12$ kPa (SD 1.19)).

245 DISCUSSION

246 This study is the first to measure muscle shear modulus in children through the use of
247 MRE technique and to study changes of the mechanical properties from childhood to
248 adulthood.

249 The increase of the muscle shear modulus with the level of contraction is in agreement
250 with the literature (Dresner et al., 2001; Basford et al., 2002; Bensamoun et al., 2006). Slight
251 differences in values may exist due to either the experimental set up (pneumatic vs.
252 mechanical driver) or the choice of frequency (90Hz vs. 120Hz). The originality of the
253 present study was to show the evolution of the shear modulus map related to the level of
254 contraction. Indeed, the mappings obtained at rest, 10% MVC and 20% MVC provided
255 information about the spatial distribution of the contracted muscle area related to the
256 physiological activity or other intrinsic muscle parameters such as the degree of anisotropy,
257 the pre-stretch of muscle fibers or connective tissue as well as the boundary conditions.
258 Stiffnesses's images were also presented by Chen et al. (2007, 2008) for upper trapezius
259 muscle affected by myofascial pain in order to visualize and to localize areas of higher
260 stiffness.

261 The behaviors of the muscle contractile properties were found to be different as a
262 function of age. At 10% MVC, individuals in their fifties as well as children have already
263 reached a maximal shear modulus compared to young adults that realize progressive muscle
264 fibers recruitment according to the degree of contraction (Bensamoun et al., 2006). Indeed,
265 the present study revealed that persons in their fifties required a more important recruitment
266 of fast fibers to reach a small level of contraction (10% MVC). Thus, the massive recruitment
267 of fibers may explain the difference (about 3kPa) in shear modulus between young and
268 middle-aged subjects. However, at a higher level of contraction (20% MVC), middle-aged

269 subjects exhibited a slight decrease of muscle stiffness that may be due to changes in muscle
270 structure (decline of the size and number of fibers) and physiology (diminution of myosin
271 protein).

272 Children showed a significant lower shear modulus at rest compared to the adult
273 groups which have similar muscle stiffness. This result demonstrated the capability of the
274 shear wave to reflect different age-related muscle media. According to the present results, it is
275 apparent that muscle structure is different during the childhood, while it is the same between
276 20 and 59 years of age. Similar results were found by Domire et al. (2009a), i.e. no significant
277 difference of shear modulus measured at rest for the tibialis anterior muscle between 50 and
278 70 years of age. This last result is surprising because aging muscle is well present at 70 years
279 of age but the effect of age may not be the same for all kinds of skeletal muscles and a larger
280 range of shear modulus may be found for oldest subjects depending of the physical condition
281 of the person at this age. For a small level of contraction (10% MVC) children demonstrated
282 the highest shear modulus values compared to adult groups. Indeed, during the growing
283 muscle process there is an on-going structural organization with the lengthening of the fibers,
284 leading to random and uncontrolled fibers recruitment (Debernard et al. 2011). As a
285 consequence, childhood muscle was unable to control progressively muscle fibers recruitment
286 to perform a small contraction, and instead contract unintentionally all the muscles fibers
287 leading to a high shear modulus. Over activation of the muscle at low activities ($< 25\%$ of
288 MVC) was also found in the literature for the triceps surae muscle of children (7 to 11 years
289 old) (Grosset et al., 2008).

290 The attenuation coefficient is a mechanical parameter reflecting the composition of the
291 muscle media. Attenuation coefficients obtained in this study for relaxed muscle were in the
292 same range as those found in the literature on the same muscle (Domire et al., 2009b). To our

293 knowledge, the present work showed the first attenuation coefficient data base for the
294 contracted state of muscle. According to the present results, it can be stated that the
295 attenuation coefficient revealed the muscle condition, with a decrease of this parameter during
296 muscle fibers stretching. Indeed, this last result could be used by clinicians to better
297 characterize neuromuscular diseases.

298

299 CONCLUSION

300 In conclusion, this study demonstrates that MRE technique is sensitive enough to
301 detect changes in contractile properties from childhood to adulthood, and it would be of
302 interest to extend this study at different age points in order to accurately follow changes
303 occurring during the growing muscle phase and aging process. Furthermore, the
304 characterization of the mechanical properties for normal children will provide muscle stiffness
305 database to clinicians in order to quantitatively assess pathological muscles and the effects of
306 treatments and therapies.

307

308

309

310

311

312

313

314

315

316

317

318

319

320

321

322

323 **ACKNOWLEDGEMENT**

324 This work was supported by the Association Française contre les Myopathies (AFM) and the
325 Picardie Region.

326

327 **REFERENCES**

- 328 Akima, H., Kanq, Y., Enomoto, Y., Ishizu, M., Okada, M., Oishi, Y., et al., 2001. Muscle
329 function in 164 men and women aged 20--84 yr. *Med Sci Sports Exerc*, 33, 220-6.
- 330 Basford, J.R., Jenkyn, T.R., An, K.N., Ehman, R.L., Heers, G., Kaufman, K.R., 2002.
331 Evaluation of healthy and diseased muscle with magnetic resonance elastography. *Arch Phys*
332 *Med Rehabil*, 83, 1530-6.
- 333 Bensamoun, S.F., Ringleb, S.I., Littrell, L., Chen, Q., Brennan, M., Ehman, R.L. et al., 2006.
334 Determination of thigh muscle stiffness using magnetic resonance elastography. *J Magn*
335 *Reson Imaging*, 23, 242-7.
- 336 Bensamoun, S.F., Ringleb, S.I., Chen, Q., Ehman, R.L., An, K.N., Brennan, M., 2007. Thigh
337 muscle stiffness assessed with magnetic resonance elastography in hyperthyroid patients
338 before and after medical treatment. *J Magn Reson Imaging*, 26, 708-13.
- 339 Brauck, K., Galban, C.J., Maderwald, S., Herrmann, B.L., Ladd, M.E., 2007. Changes in calf
340 muscle elasticity in hypogonadal males before and after testosterone substitution as monitored
341 by magnetic resonance elastography. *Eur J Endocrinol*, 156, 673-8.
- 342 Chen, Q., Bensamoun, S., Basford, J.R., Thompson, J.M., An, K.N., 2007. Identification and
343 quantification of myofascial taut bands with magnetic resonance elastography. *Arch Phys*
344 *Med Rehabil*, 88, 1658-61.
- 345 Chen, Q., Basford, J., An, K.N., 2008. Ability of magnetic resonance elastography to assess
346 taut bands. *Clin Biomech (Bristol, Avon)*, 23, 623-9.
- 347 Debernard, L., Robert, L., Charleux, F., Bensamoun, S.F., 2011. Characterization of muscle
348 architecture in children and adults using magnetic resonance elastography and ultrasound
349 techniques. *J Biomech*, 44, 397-401.

350

- 351 Domire, Z.J., Mccullough, M.B., Chen, Q., An, K.N., 2009a. Feasibility of using magnetic
352 resonance elastography to study the effect of aging on shear modulus of skeletal muscle. *J*
353 *Appl Biomech*, 25, 93-7.
- 354 Domire, Z.J., Mccullough, M.B., Chen, Q., An, K.N., 2009b. Wave attenuation as a measure
355 of muscle quality as measured by magnetic resonance elastography: initial results. *J Biomech*,
356 42, 537-40.
- 357 Dresner, M.A., Rose, G.H., Rossman, P.J., Muthupillai, R., Manduca, A., Ehman, R.L., 2001.
358 Magnetic resonance elastography of skeletal muscle. *J Magn Reson Imaging*, 13, 269-76.
- 359 Grosset, J.F., Mora, I., Lambertz, D., Perot, C., 2008. Voluntary activation of the triceps surae
360 in prepubertal children. *J Electromyogr Kinesiol*, 18, 455-65.
- 361 Heckmatt, J.Z., Pier, N., Dubowitz, V., 1988. Assessment of quadriceps femoris muscle
362 atrophy and hypertrophy in neuromuscular disease in children. *J Clin Ultrasound*, 16, 177-81.
- 363 Kamala, D., Suresh, S., Githa, K., 1985. Real-time ultrasonography in neuromuscular
364 problems in children. *J Clin Ultrasound*, 13, 465-8
- 365 Lamminen, A., Jaaskelainen, J., Rapola, J., Suramo, I., 1988. High-frequency ultrasonography
366 of skeletal muscle in children with neuromuscular disease. *J Ultrasound Med*, 7, 505-9.
- 367 Lynch, N.A., Metter, E.J., Lindle, R.S., Fozard, J.L., Tobin, J.D., Roy, T.A., et al., 1999.
368 Muscle quality. I. Age-associated differences between arm and leg muscle groups. *J Appl*
369 *Physiol*, 86, 188-94.
- 370 Manduca, A., Oliphant, T.E., Dresner, M.A., Mahowald, J.L., Kruse, S.A., Amromin, E., et
371 al., 2001. Magnetic resonance elastography: non-invasive mapping of tissue elasticity. *Med*
372 *Image Anal*, 5, 237-54.
- 373 Pillen, S., Verrips, A., Van Alfen, N., Arts, I.M., Sie, L.T., Zwarts, M.J., 2007. Quantitative
374 skeletal muscle ultrasound: diagnostic value in childhood neuromuscular disease.
375 *Neuromuscul Disord*, 17, 509-16.

376 Schedel, H., Reimers, C.D., Nagele, M., Witt, T.N., Pongratz, D.E., Vogl, T., 1992. Imaging
377 techniques in myotonic dystrophy. A comparative study of ultrasound, computed tomography
378 and magnetic resonance imaging of skeletal muscles. *Eur J Radiol*, 15, 230-8.

379 Zuberi, S.M., Matta, N., Nawaz, S., Stephenson, J.B., McWilliam, R.C., Hollman, A., 1999.
380 Muscle ultrasound in the assessment of suspected neuromuscular disease in childhood.
381 *Neuromuscul Disord*, 9, 203-7.

382

Figure Legends:

Fig. 1: A: anatomical image of the vastus medialis (VM) muscle in a relaxed state. B: Phase image with a white profile drawn along the direction of the shear wave's propagation following the path of muscle fascicle. C: Amplitude image resulting from the amplitude value of the first temporal harmonic extracted at the driven frequency 90Hz along each pixel.

Sr: Sartorius; VM: Vastus Medialis.

Fig. 2: Computation of the attenuation coefficient α (m^{-1}) from the wave displacement amplitude in function of the distance.

Fig. 3: Bar graph (A) with the corresponding data (B) of the local shear modulus (μ_{local}) measured along the propagation of the shear waves for each age points and for different VM muscle conditions (rest, 10% MVC, 20% MVC). The table (B) showed the comparison of the shear modulus measured locally (μ_{local}) and inside the region of interest (μ_{ROI}). (** $P < 0.05$ and * $P < 0.1$).

Fig. 4: Individual bar graph illustrating the VM shear modulus in relaxed and contracted (10% and 20% MVC) conditions for children (A), young adults (B) and middle-aged adults (C) (** $P < 0.05$ and * $P < 0.1$).

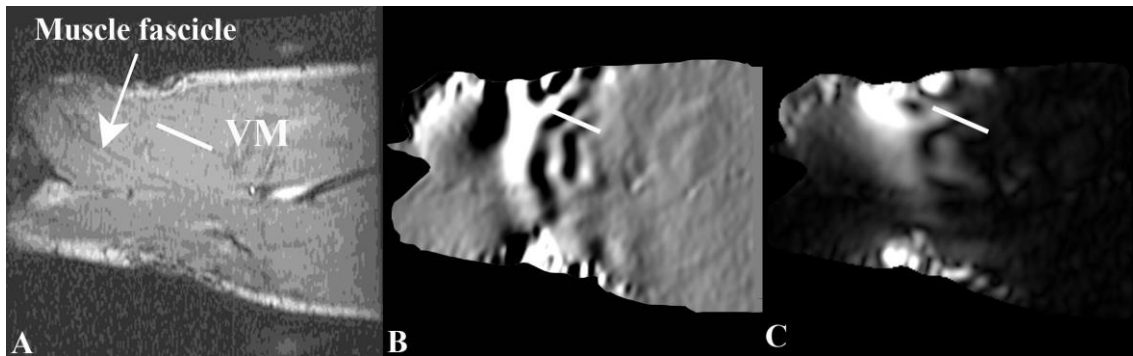
Fig. 5: Bar graph (A) with the corresponding table (B) illustrating the attenuation coefficient (α) in relaxed and contracted (10% and 20% MVC) states for children, young and middle-aged adults (** $P < 0.05$ and * $P < 0.1$).

407 **Fig. 6:** Mapping of shear modulus for the VM at rest and contracted (10% and 20% of MVC)
408 conditions for the children, young and middle-aged adults. Muscle stiffness was analysed
409 inside the prescribed region of interest (ROI), placed around the red profil for each group and
410 each muscle state.

411

412

413 **Figures:**

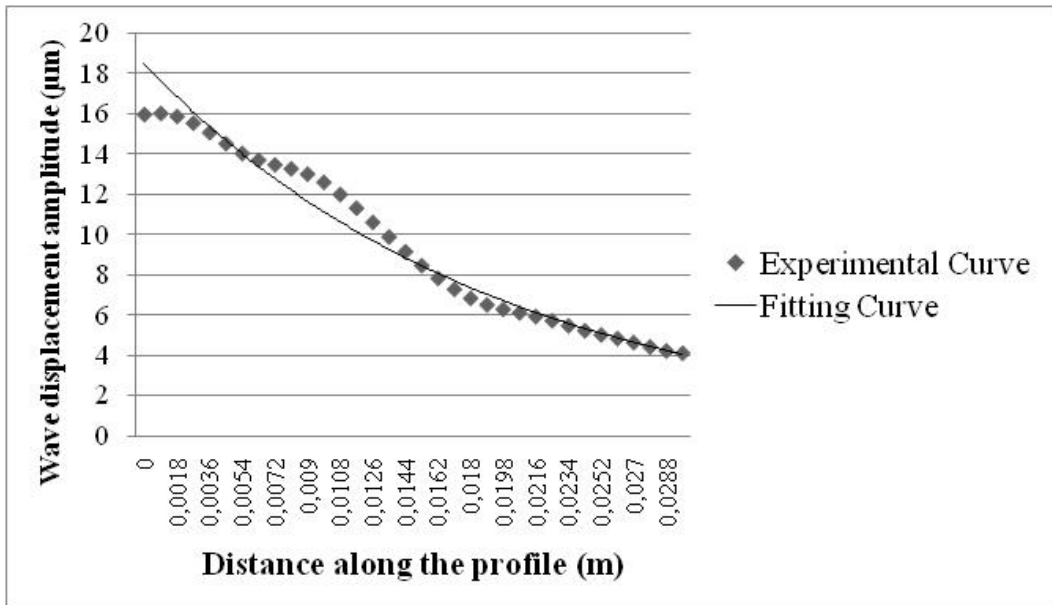


414

415 **Fig. 1:** A: anatomical image of the vastus medialis (VM) muscle in a relaxed state. B: Phase
416 image with a white profile drawn along the direction of the shear wave's propagation
417 following the path of muscle fascicle. C: Amplitude image resulting from the amplitude value
418 of the first temporal harmonic extracted at the driven frequency 90Hz along each pixel.

419 Sr: Sartorius; VM: Vastus Medialis.

420

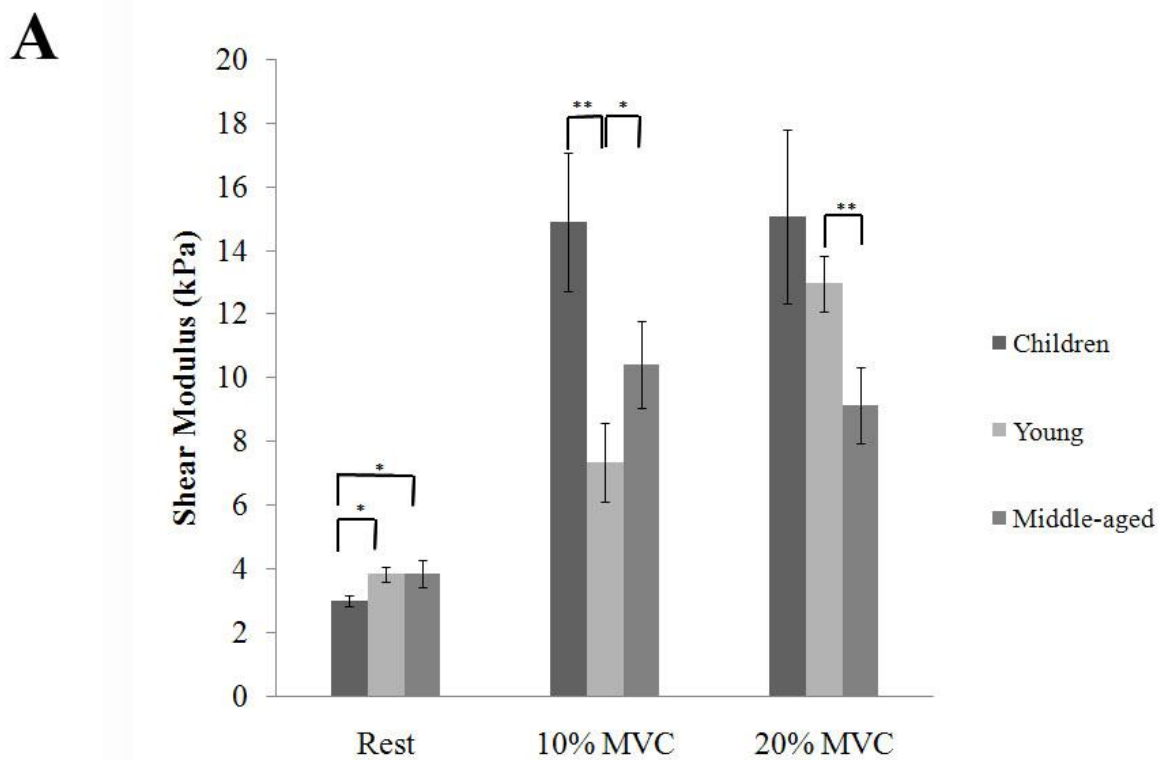


421

422 **Fig. 2:** Computation of the attenuation coefficient α (m^{-1}) from the wave displacement
423 amplitude in function of the distance.

424

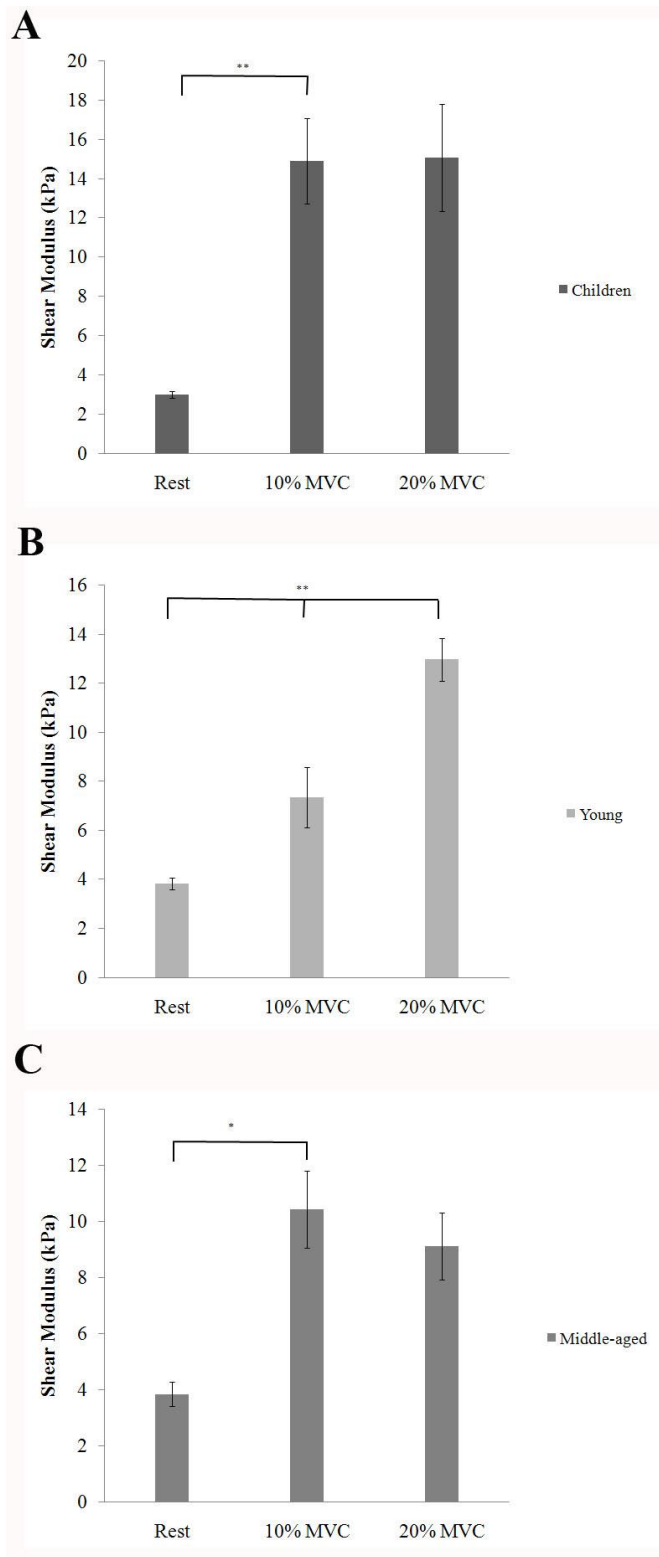
425

**B**

	REST		10%MVC		20%MVC	
	μ_{Local} (kPa)	μ_{ROI} (kPa)	μ_{Local} (kPa)	μ_{ROI} (kPa)	μ_{Local} (kPa)	μ_{ROI} (kPa)
Children	2.99 ± 0.19	3.61 ± 0.27	14.9 ± 2.18	12.4 ± 1.36	15.05 ± 2.73	13.3 ± 2.03
Young Adults	3.83 ± 0.24	4.14 ± 0.26	7.33 ± 1.23	7.46 ± 0.85	12.97 ± 0.87	11.9 ± 1.38
Middle-aged adults	3.84 ± 0.42	3.2 ± 0.48	10.42 ± 1.38	10.7 ± 2.08	9.12 ± 1.19	8.53 ± 2.01

426

427 **Fig. 3:** Bar graph (A) with the corresponding data (B) of the local shear modulus (μ_{local})
 428 measured along the propagation of the shear waves for each age points and for different VM
 429 muscle conditions (rest, 10% MVC, 20% MVC). The table (B) showed the comparison of the
 430 shear modulus measured locally (μ_{local}) and inside the region of interest (μ_{ROI}). (** $P < 0.05$
 431 and * $P < 0.1$).

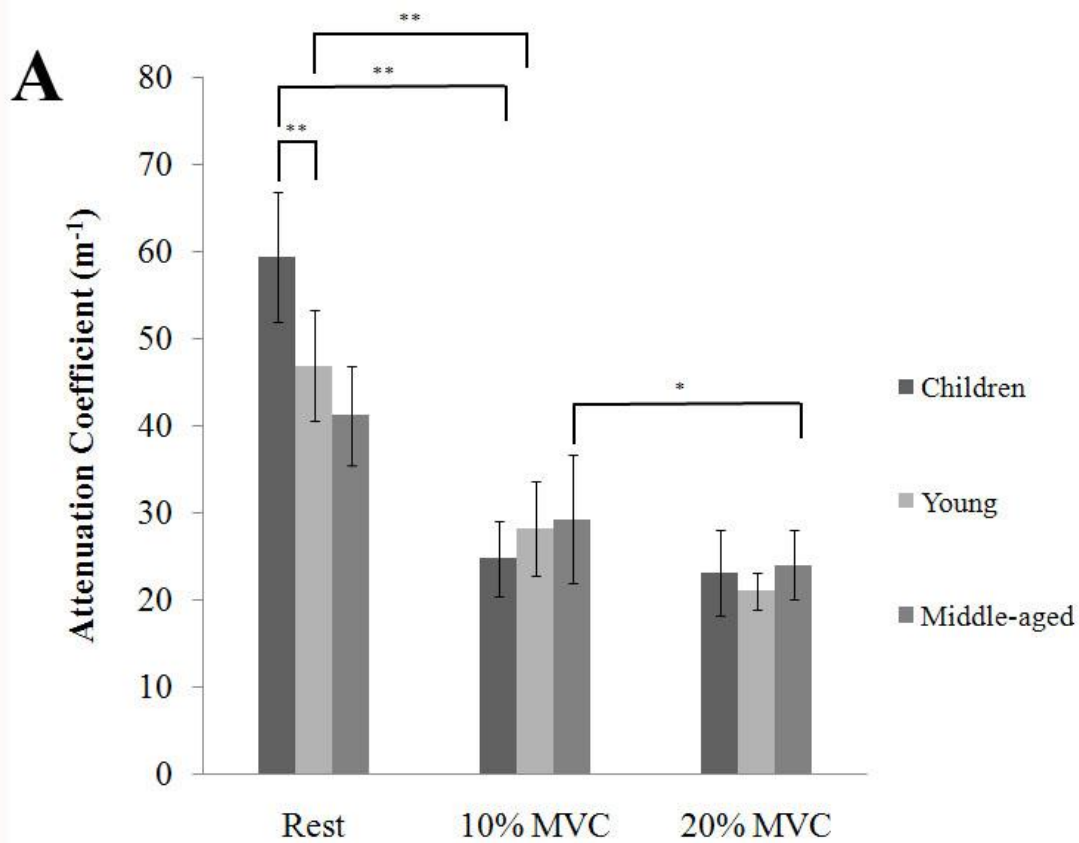


432

433 **Fig. 4:** Individual bar graph illustrating the VM shear modulus in relaxed and contracted (10%

434 and 20% MVC) conditions for children (A), young adults (B) and middle-aged adults (C) (**

435 $P < 0.05$ and $*P < 0.1$).



B

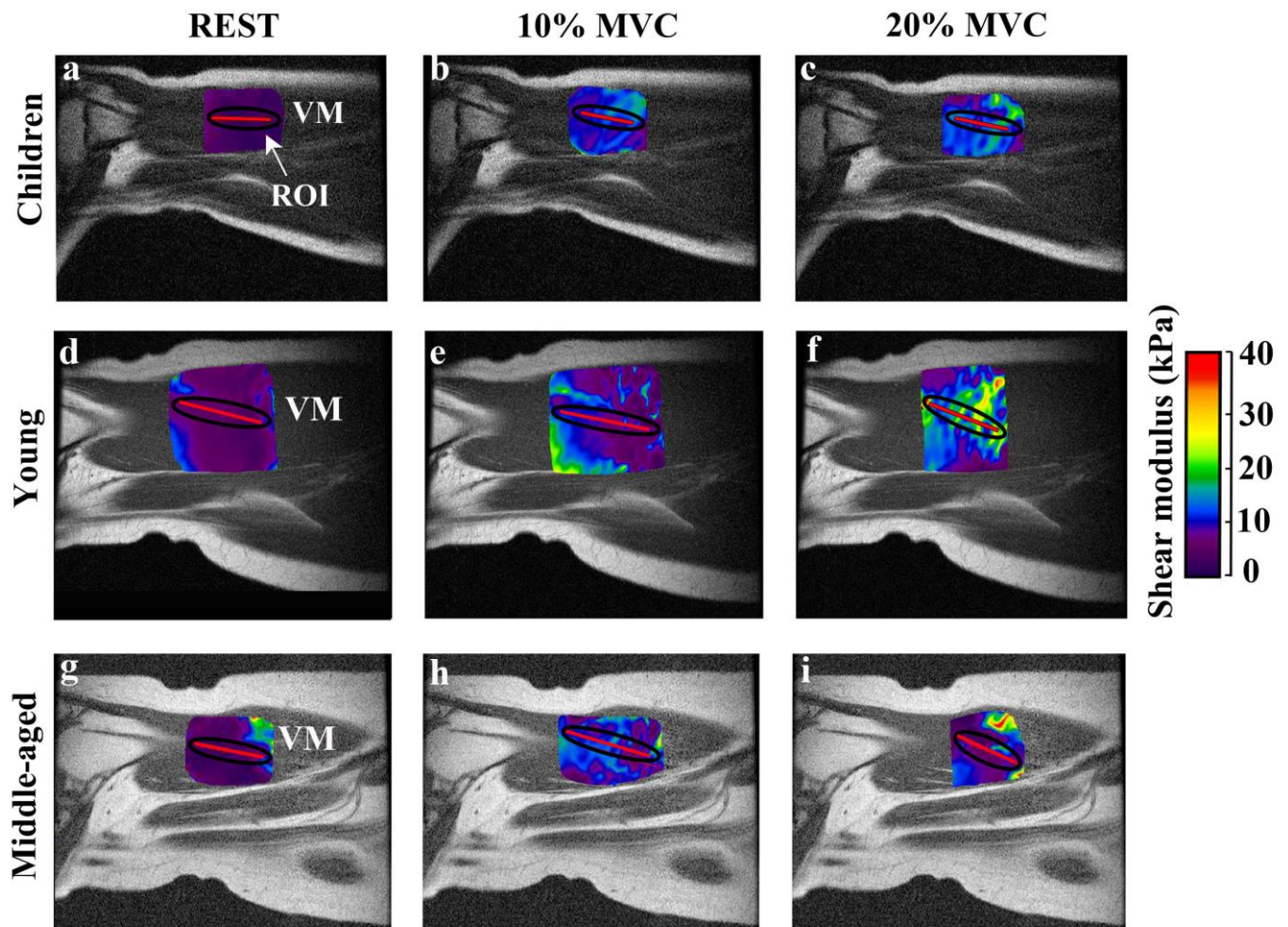
	Attenuation coefficient (m^{-1})		
	REST	10%MVC	20%MVC
Children	59.43 ± 7.44	24.71 ± 4.31	23.17 ± 4.91
Young Adults	46.89 ± 6.35	28.14 ± 5.42	21 ± 2.13
Middle-aged adults	41.2 ± 5.68	29.2 ± 7.37	24 ± 3.93

436

437 **Fig. 5:** Bar graph (A) with the corresponding table (B) illustrating the attenuation coefficient

438 (α) in relaxed and contracted (10% and 20% MVC) states for children, young and middle-

439 aged adults (** $P < 0.05$ and * $P < 0.1$).



440

441 **Fig. 6:** Mapping of shear modulus for the VM at rest and contracted (10% and 20% of MVC)
 442 conditions for the children, young and middle-aged adults. Muscle stiffness was analysed
 443 inside the prescribed region of interest (ROI), placed around the red profil for each group and
 444 each muscle state.